ELSEVIER

Synthetic Metals 139 (2003) 695–700

SYNTHETIC METALS

www.elsevier.com/locate/synmet

Optical properties and photonic mode dispersion in two-dimensional and waveguide-embedded photonic crystals

L.C. Andreani [a,*], M. Agio [a], D. Bajoni [a], M. Belotti [a], M. Galli [a], G. Guizzetti [a], A.M. Malvezzi [b], F. Marabelli [a], M. Patrini [a], G. Vecchi [a]

[a] *Istituto Nazionale per la Fisica della Materia (INFM) and Dipartimento di Fisica "A. Volta", Università degli Studi di Pavia, via Bassi 6, I-27100 Pavia, Italy*

[b] *Istituto Nazionale per la Fisica della Materia (INFM) and Dipartimento di Elettronica, Università degli Studi di Pavia, via Ferrata 1, I-27100 Pavia, Italy*

Abstract

Recent experimental and theoretical work on two-dimensional (2D) and waveguide-embedded photonic crystals is reviewed. The investigated systems are 2D macroporous silicon and photonic crystal slabs based on silicon-on-insulator as well as GaAs/AlGaAs. In all these structures, reflectance at varying angles of incidence allows to determine the dispersion of photonic modes above the light line. For macroporous silicon, reflectance from the side yields a complementary measurement of the photonic gaps. In the GaAs-based system, second-harmonic generation in reflection shows a resonant enhancement when the pump beam is frequency- and momentum-matched to a photonic mode in the slab. A theory of photonic states in waveguide-embedded photonic crystals leads to a determination of mode dispersion and diffraction losses for leaky photonic modes.

Keywords: Photonic crystals; Silicon; GaAs/AlGaAs; Optical waveguides; Optical properties; Second-harmonic generation

1. Introduction

Photonic crystals are materials whose dielectric constant is periodic in one, two, or three dimensions. They were first proposed by Yablonovitch [1] and John [2] as a way to suppress spontaneous emission and to localize light by disorder. The spatial periodicity leads to Bloch–Floquet theorem and to the existence of *photonic bands*, which are analogous to electron bands in crystalline solids. A frequency region in which photons cannot propagate is called a *photonic gap*.

Three-dimensional (3D) photonic crystals may possess a complete band gap for all propagation directions and polarizations [3,4], yet they are not easy to realize at near-infrared and optical wavelengths. Moreover, self-assembled structures like direct and inverse opals are obtained through a bottom-up approach, which is not suitable for introducing linear and point defects in a controlled way. 2D photonic crystals, on the other hand, can be realized at optical wavelengths by top-down approaches based on lithography and etching: the fabrication procedure allows to introduce linear defects (acting as channel waveguides, perhaps with sharp bends) or point defects (acting as microcavities) at the level of the lithographic mask.

The prototype of a 2D photonic crystal is macroporous silicon [5]. 2D photonic structures can also be embedded in planar waveguides, thereby realizing the so-called *photonic crystal slabs* [6,7]: they have the advantage that propagation of light is controlled by the photonic structure in the 2D (xy) plane, and by the refractive index discontinuity of the slab waveguide in the vertical (z) direction. However, modes lying above the light line in photonic crystal slabs are subject to radiation losses due to diffraction out of the plane.

In this paper, recent experimental and theoretical work on 2D and waveguide-embedded photonic crystals is reviewed [8–18]. We consider 2D macroporous silicon (Section 2) and photonic crystal slabs based on silicon-on-insulator (SOI) as well as GaAs/AlGaAs (Section 3). In Section 4, we describe a theoretical model which allows to calculate the dispersion of modes in photonic crystal slabs, both below and above the light line, as well as diffraction losses of radiative photonic modes.

* Corresponding author. Tel.: +39-0382-507491; fax: +39-0382-507563.
E-mail address: andreani@fisicavolta.unipv.it (L.C. Andreani).

0379-6779/$ – see front matter © 2003 Elsevier B.V. All rights reserved.
doi:10.1016/S0379-6779(03)00330-8

2. Two-dimensional photonic crystals: macroporous silicon

Macroporous silicon is obtained by anodic dissolution of Si in an electrochemical cell. A regular lattice of etch pits is first defined on the sample surface by optical or electron-beam lithography; subsequently, a wet etching procedure yields macropores up to 50–100 μm deep. Since the pore depth is much larger than the wavelength of light, the photonic crystal can be considered as homogeneous in the vertical direction and can be viewed as two-dimensional. Macroporous silicon can be realized on n-type [5,8] as well as on p-type substrates [9].

Transmittance measurements in the 2D plane yield a direct determination of the gap energy window and of the attenuation as a function of thickness [5], however, they require the sample to be cut from both sides and to be a few period thick. As an alternative, the sample can be cleaved on one side only and the reflectance can be measured with conventional microscope optics combined with Fourier transform infrared spectroscopy [9]. In Fig. 1a, we show the normal incidence reflectance from the side of a macroporous Si sample patterned with a triangular lattice of holes, and in Fig. 1b, the corresponding photonic bands: both are taken along the ΓM direction of the 2D Brillouin zone and for E polarization (electric field along the pore axis z). The measured reflectance is very well reproduced by the results of a calculation, in which the electromagnetic field in the photonic crystal is represented by Bloch modes of the periodic structure, which are matched to the external field by Maxwell boundary conditions. Only modes that are even with respect to a vertical mirror plane are considered (solid lines in Fig. 1b), as appropriate to normally incident light with E polarization. When more than one Bloch mode propagates at a given frequency, only the one yielding the larger transmission coefficient is kept. The maxima of the reflectance correspond very well to the photonic gaps in the mode dispersion, considering that only even modes are probed.

Transmittance or reflectance measurements from the side yield the *photonic gaps*, but not the *mode dispersion*. The latter can be determined from variable-angle reflectance from the sample surface, as first shown in [19] on photonic crystal waveguides: when the incident beam has the same frequency ω and in-plane wavevector $k_{\parallel}$ of a photonic mode along a given orientation (i.e. when $k_{\parallel} = (\omega/c)\sin\theta$, where θ is the angle of incidence), a diffracted beam is generated in the material and a corresponding spectral structure appears in the reflectance spectrum. The angular evolution of the spectral structures yields the dispersion of photonic modes lying above the light dispersion in air. In Fig. 2a, we show variable-angle reflectance spectra taken on a macroporous silicon sample, again with a triangular pattern of holes. It can be seen [8] that even if the sample is homogeneous along the vertical direction (i.e. no waveguide is present), well-defined structures show up in reflectance spectra and have a regular behavior as a function of θ. The photonic band dispersion in the first Brillouin zone is shown in Fig. 2b: good agreement between experiment and theory is found in a wide energy window. Since the 2D photonic crystal retains an out-of-plane dispersion in the z-direction, each spectral structure in reflectance marks the *threshold* for the excitation of a photonic mode and it is shown to correspond to a critical point of 1D type [8].

Looking at the intensities of reflectance structures in Fig. 2a, it is interesting to observe that most of them become vanishingly weak at near-normal incidence, with the exception of a strong structure near 0.3 eV. This and other features can be understood by a symmetry analysis combined

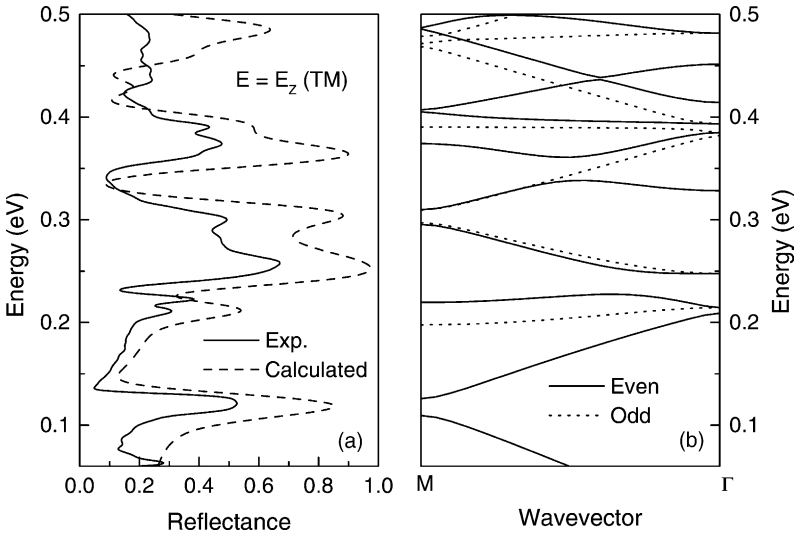

Fig. 1. (a) Experimental and theoretical reflectance from the side of a macroporous silicon sample for TM polarization (electric field along the z-direction); (b) corresponding E-polarized photonic bands. The sample, which is patterned with a triangular lattice of holes with 2 μm period and 28% air fraction, is cut along the ΓK direction; therefore, the reflectance and the bands are along the ΓM direction of the Brillouin zone. The theoretical spectrum in (a) includes a Gaussian broadening of 8 meV.

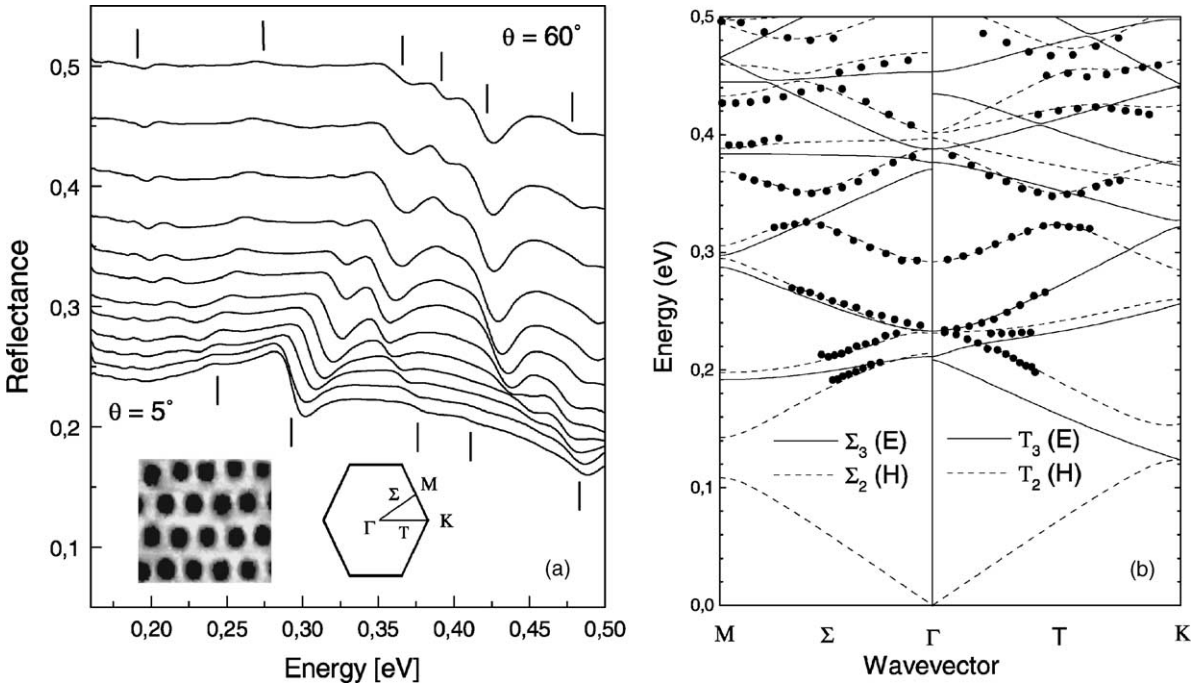

Fig. 2. (a) Reflectance of a macroporous silicon sample for TE-polarized light incident along the ΓM orientation. The angle of incidence θ is varied from 5 to 60° in steps of 5°. The curves at 5, 10 and 15° are slightly offset for clarity. Vertical bars mark the positions of 2D photonic modes for 5 and 60°. Insets: AFM micrograph of the sample (dimensions: 10 μm × 8.4 μm) and 2D Brillouin zone. (b) Measured (points) and calculated (lines) dispersion of the photonic bands for TE polarization (odd modes). The sample is patterned with a triangular lattice of holes with 2 μm period and 30% air fraction.

with the following selection rule: *a photonic mode can appear in reflectance only if it has the same symmetry of the incident beam*. The strong feature around 0.3 eV corresponds indeed to a mode with dipolar symmetry at the Γ point. At oblique incidence, the incoming beam couples to both E and H modes of the photonic structure: in addition, for an orientation along a symmetry direction of the Brillouin zone photonic modes may and should be classified according to mirror symmetry with respect to the plane of incidence. In a sense, variable-angle reflectance from the crystal surface has analogies to spectroscopic studies of electronic or vibrational excitations in solids—it may be called "*spectroscopy of photonic modes*".

3. Waveguide-embedded photonic crystals: silicon-on-insulator, GaAs/AlGaAs

Silicon-on-insulator photonic crystal slabs consist of a Si core layer on top of a SiO_2 lower cladding: thanks to the large dielectric contrast between core and cladding, only the Si layer need to be patterned. The fabrication procedure is based on electron-beam lithography and reactive-ion etching with fluorine chemistry [11]. The high control of processing in the Si/SiO_2 system makes SOI photonic crystal slabs very attractive for the realization of passive optical interconnects.

Fig. 3 shows TE-polarized variable-angle reflectance spectra and the corresponding photonic bands of a 1D lattice patterned in a SOI waveguide [10]. Well-defined spectral structures with a smooth angular evolution are visible: their identification is simplified by comparing experimental spectra with those theoretically calculated by a scattering matrix approach [20]. An anticrossing of modes around 0.9 eV can be recognized. The measurements give direct evidence of a gap around 0.75 eV ($\lambda = 1.65$ μm): the band dispersion identifies it as a second-order gap, i.e. a gap at the Γ point in the first Brillouin zone. Only photonic modes lying above the light dispersion in air (dashed line in Fig. 3b) are probed by reflectance from the surface. The anticrossing of modes at 0.9 eV, as well as similar features at higher energies, are seen to correspond to coupling between a first-order waveguide mode and a second-order one whose cutoff energy is just above 0.8 eV.

The solid lines in Fig. 3b represent the dispersion of photonic modes calculated by a finite-basis expansion method (see Section 4). Modes that lie below the light lines of the two claddings are *truly guided modes* of the photonic crystal slab, while those lying above the light line should be viewed as resonances, or *quasi-guided modes*, since they are subject to radiative losses corresponding to out-of-plane diffraction. In fact, the resonances in Fig. 3a appear because of the reverse mechanism, namely the generation of a quasi-guided mode in the slab due to diffraction of the incident beam. The calculated dispersion of quasi-guided modes is in very good agreement with the experimental results: of course, frequency dispersion of the dielectric functions (especially for Si) is essential and has been taken into account.

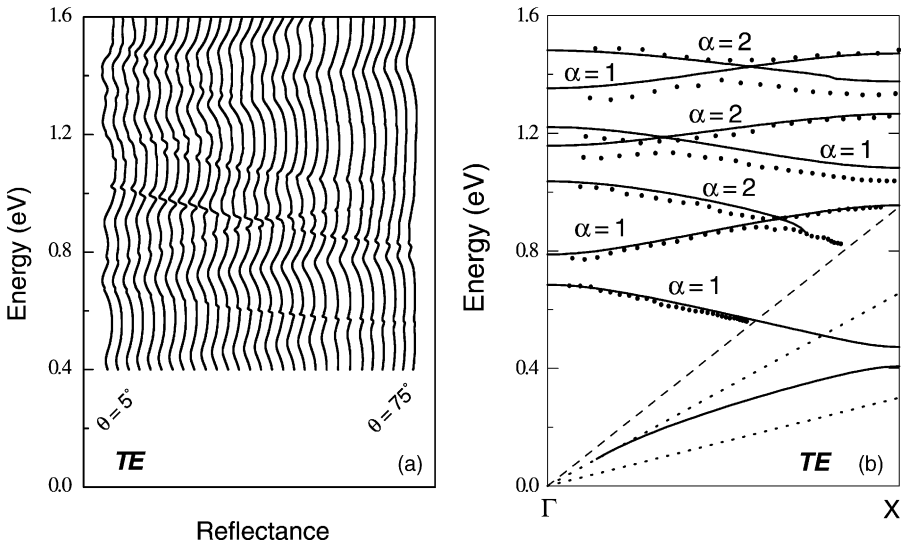

Fig. 3. (a) TE-polarized reflectance spectra from 5 to 75° in steps of 2.5° of a SOI photonic crystal slab patterned with a 1D lattice with 0.65 μm period and 18% air fraction (the curves are offset for clarity); (b) corresponding photonic bands for odd (TE) modes, as measured from the reflectance (points) and calculated (solid lines). The dashed (dotted) lines in (b) indicate the dispersion of light in air (SiO_2 and Si).

GaAs/AlGaAs photonic crystal slabs are based on a planar waveguide with low refractive index contrast, therefore both core and claddings need to be patterned. The preparation procedure usually involves electron-beam lithography followed by reactive-ion etching with chlorine chemistry; in [13], X-ray lithography was also used. Variable-angle reflectance measurements on samples with square lattices lead again to the determination of the photonic mode dispersion above the light line and to the study of selection rules and symmetry properties [12].

A particularly interesting feature of III–V-based systems is their second-order susceptibility $\chi^{(2)}$ arising from the lack of inversion symmetry of the zinc blende lattice: they are therefore suitable for non-linear studies like second-harmonic generation (SHG). Malvezzi et al. [14] described SHG measurements on GaAs/AlGaAs photonic crystal slabs in reflection and diffraction geometries: in particular, the observation of *second-harmonic diffraction* is reported. The latter is a coherent process whereby the laser pulse generates a second-harmonic beam, which is at the same time diffracted by the grating. Also, resonance effects are expected when the pump and/or the second-harmonic beam are frequency- and momentum-matched to photonic modes in the slab [21]. The experimental observation of the resonance effect of the pump beam is reported in Fig. 4, which shows the SH reflection signal for different pump wavelengths as a function of the azimuthal angle, i.e. the rotation angle of the sample around its normal. Eight sharp peaks are seen to occur in each full turn, due to the four-fold rotational symmetry of the square photonic lattice and to the fact that each photonic band is crossed twice in each 90° irreducible portion of the 2D Brillouin zone. Each pair of peaks has a regular evolution as a function of pump wavelength: this allows mapping the photonic band dispersion with an increased sensitivity compared to linear spectra [15]. Moreover, the SH structures associated to the excitation of photonic modes have always the form of resonant peaks, i.e. photonic modes lead to en *enhancement* of SHG. The reason lies partly in the strong increase of the electric field strength in the core layer when a mode is excited, and partly in the very nature of SHG which arises

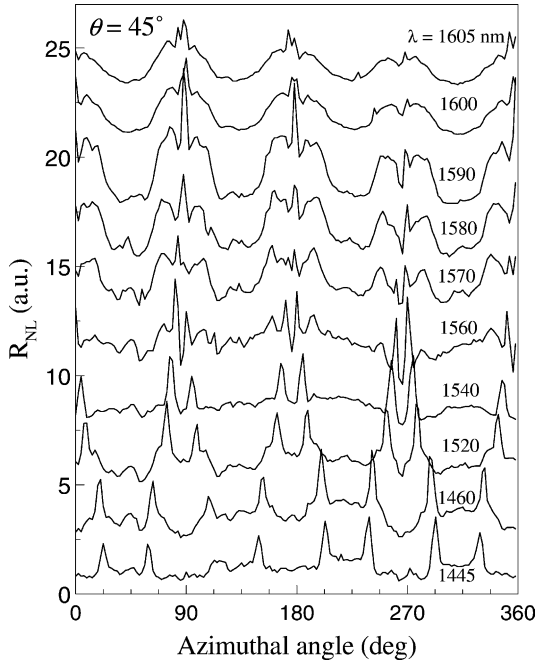

Fig. 4. Non-linear reflectance vs. azimuthal angle ϕ (at $\theta = 45°$, TM polarization of the pump) of a GaAs/AlGaAs photonic crystal slab at different pump wavelengths. The curves are offset for clarity. The sample has a square lattice of tilted air rings with 0.5 μm period and 12% air fraction.

from a non-linear polarization producing a source field in the non-linear medium: SHG generation can be viewed as an "emission" process due to the source field, thus its spectral lineshape reflects the natural linewidth of the resonance involved (unlike linear reflectance, in which a photonic mode can appear with widely different lineshapes including dispersive ones). This allows in principle to measure the *radiative linewidth* of photonic modes and therefore their intrinsic diffraction losses from SHG. The resonance effect shown in Fig. 4 is weaker than predicted [21], due to the spectral width of the 130 fs laser pulse as well as to sample inhomogeneity: still, photonic-mode enhancement of SHG has interesting prospects both for exploiting resonance effects and as a non-linear spectroscopic tool for optical studies of photonic crystals.

4. Mode dispersion and radiative losses in photonic crystal slabs

While the energies of guided modes in photonic crystal slabs can be calculated by introducing a supercell in the vertical direction and using 3D plane-wave expansion [22], the frequency dispersion and especially the losses (i.e. the imaginary part of the frequency) of quasi-guided modes are more difficult to obtain and are often calculated by numerical simulation with the finite-difference time domain technique. We follow an alternative approach [16–18], which consists on expanding the magnetic field on the basis of guided modes of an effective homogeneous waveguide, whose dielectric constants are given by the spatial average of the position-dependent dielectric constant in each layer. The second-order equation for the magnetic field is transformed into a linear eigenvalue problem, which can be solved numerically to obtain the photonic-mode energies as well as the field profiles. The off-diagonal components of the dielectric matrix $\varepsilon(\boldsymbol{G}, \boldsymbol{G}')$ lead to a folding of photonic modes in the first Brillouin zone and to a splitting of degenerate eigenmodes, resulting in the formation of photonic bands and gaps. The method is a generalization of usual plane-wave expansion in 2D, the third dimension being taken into account by the spatial dependence of the guided modes of the effective waveguide. When the photonic modes folded in the first Brillouin zone fall above the light line of the cladding material (or materials, if the waveguide is asymmetric), they become quasi-guided. The imaginary part of the complex frequency of quasi-guided modes is computed by taking into account coupling of guided modes to leaky modes of the effective waveguide by Fermi's Golden Rule.

An example of complex frequency dispersion is given in Fig. 5, which shows the real and imaginary parts as a function of wavevector and compares them to the calculated reflectance at various angles of incidence. The *energy positions* of the spectral features in reflectance as a function of incidence angle are seen to correspond to the wavevector dispersion of the *real part of the frequency* (Fig. 5a). The *linewidths* of the resonances also change with the incidence angle and correspond to the *imaginary part of the frequency* shown in Fig. 5c: for example, the first even band has a linewidth which increases as a function of wavevector (until

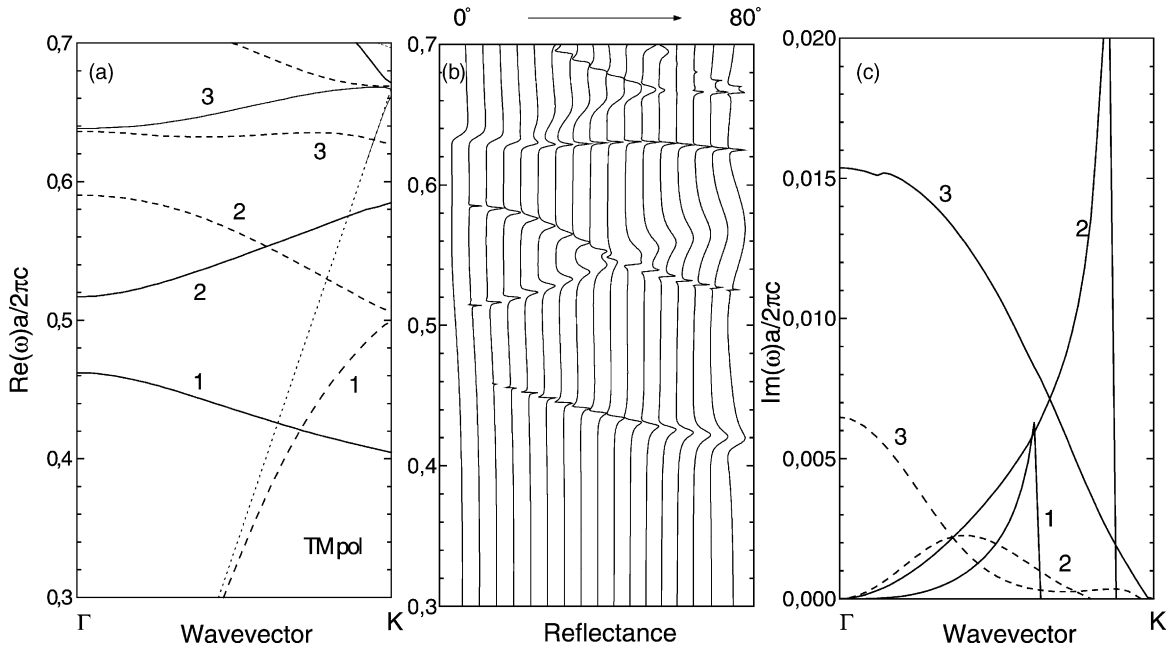

Fig. 5. (a) Photonic mode dispersion (real part of energy), (b) reflectance spectra from 0 to 80° in steps of 5°, and (c) imaginary part of energy calculated for a self-standing membrane with $\varepsilon = 12$, patterned with a triangular lattice of holes with 32.6% air fraction. All curves are calculated for TM polarized modes along the ΓK orientation. Solid (dashed) lines refer to even (odd) modes with respect to a horizontal mirror plane. The dotted line in (a) is the light line in air.

it drops to zero at the light cone), whereas the third even band has a finite linewidth at $k_{\|} = 0$ (indeed it has dipolar symmetry at the Γ point) which decreases as a function of wavevector. These and other features can be recognized in the reflectance curves in Fig. 5b.

A few applications of the method to calculating photonic bands, gap maps and radiative losses for the triangular lattice of holes are discussed in [16,17]. The model may also used for calculating the photonic dispersion and the intrinsic losses for defect modes associated to channel waveguides, like the so-called W1 waveguide (i.e. a single missing row of holes along the ΓK direction in the triangular lattice) [18]. The imaginary parts and the propagation losses are found to be strongly dependent on the wavevector and on the precise structural parameters: generally, however, they tend to increase with the air fraction of the triangular lattice and to decrease on increasing either the channel width or the core thickness of the planar waveguide.

5. Conclusions

Photonic modes are viewed here as "elementary excitations" of the system that are probed by external photons, very much like elementary excitations (vibrational or electronic) in crystalline solids are studied by spectroscopic means. Reflectance from the side, variable-angle reflectance from the sample surface, second-harmonic generation yield complementary information that allows reconstructing the photonic gaps and mode dispersion. Photonic crystal slabs support both truly guided and quasi-guided modes: the latter are characterized by a complex frequency, which can be probed by the energy positions and linewidths of reflectance structures. A thorough understanding of the photonic band structure is a basic piece of knowledge before studying more complex problems like radiation–matter interaction (e.g. spontaneous emission control), other kinds of elementary excitations (plasmons, polaritons) or non-linear optical properties like phase-matching conditions or non-linear switching. All these problems are likely to be very active areas of research in the near future.

Acknowledgements

The authors are indebted with several partners for the fabrication of samples. Macroporous silicon photonic crystals were prepared by L. Pavesi, P. Bettotti, L. Dal Negro, Z. Gaburro, A. Lui, P. Bellutti at the University and IRST-ITC of Trento. GaAs-based photonic crystal slabs were realized by E. Di Fabrizio, F. Romanato, L. Businaro at TASC-NNL-INFM, Trieste, and by M. De Vittorio and A. Passaseo at NNL-INFM and University of Lecce. Silicon-on-insulator photonic crystal slabs were fabricated by Y. Chen and D. Peyrade at LPN-CNRS, Marcoussis, France. This work was supported by MIUR through Cofin 2000 and 2002 programs and by INFM through PAIS 2001 and PRA 2002 projects.

References

[1] E. Yablonovitch, Phys. Rev. Lett. 58 (1987) 2059.
[2] S. John, Phys. Rev. Lett. 58 (1987) 2486.
[3] J.D. Joannopoulos, R.D. Meade, J.N. Winn, Photonic Crystals—Molding the Flow of Light, Princeton University Press, Princeton, NJ, 1995.
[4] K. Sakoda, Optical Properties of Photonic Crystals, Springer, Berlin, 2001.
[5] A. Birner, R.B. Wehrspohn, U. Gösele, K. Busch, Adv. Mater. 13 (2001) 377.
[6] T.F. Krauss, R.M. De La Rue, S. Brand, Nature 383 (1996) 699.
[7] D. Labilloy, H. Benisty, C. Weisbuch, T.F. Krauss, R.M. De La Rue, V. Bardinal, R. Houdré, U. Oesterle, D. Cassagne, C. Jouanin, Phys. Rev. Lett. 79 (1997) 4147.
[8] M. Galli, M. Agio, L.C. Andreani, M. Belotti, G. Guizzetti, F. Marabelli, M. Patrini, P. Bettotti, L. Dal Negro, Z. Gaburro, L. Pavesi, A. Lui, P. Bellutti, Phys. Rev. B 65 (2002) 113111.
[9] P. Bettotti, L. Dal Negro, Z. Gaburro, L. Pavesi, A. Lui, M. Galli, M. Patrini, F. Marabelli, J. Appl. Phys. 92 (2002) 6966.
[10] M. Patrini, M. Galli, F. Marabelli, M. Agio, L.C. Andreani, D. Peyrade, Y. Chen, IEEE J. Quantum Electron. 38 (2002) 885.
[11] D. Peyrade, Y. Chen, A. Talneau, M. Patrini, M. Galli, F. Marabelli, M. Agio, L.C. Andreani, E. Silberstein, P. Lalanne, Microelectron. Eng. 61–62 (2002) 529.
[12] M. Galli, M. Agio, L.C. Andreani, L. Atzeni, D. Bajoni, G. Guizzetti, L. Businaro, E. Di Fabrizio, F. Romanato, A. Passaseo, Eur. Phys. J. B 27 (2002) 79.
[13] F. Romanato, L. Businaro, E. Di Fabrizio, A. Passaseo, M. De Vittorio, R. Cingolani, M. Patrini, M. Galli, D. Bajoni, L.C. Andreani, F. Giacometti, M. Gentili, D. Peyrade, Y. Chen, Nanotechnology 13 (2002) 644.
[14] M. Malvezzi, F. Cattaneo, G. Vecchi, M. Falasconi, G. Guizzetti, L.C. Andreani, L. Businaro, F. Romanato, E. Di Fabrizio, A. Passaseo, M. De Vittorio, J. Opt. Soc. Am. B 19 (2002) 2122.
[15] L.C. Andreani, F. Cattaneo, G. Guizzetti, A.M. Malvezzi, M. Patrini, G. Vecchi, F. Romanato, L. Businaro, E. Di Fabrizio, A. Passaseo, M. De Vittorio, Physica E, in press.
[16] L.C. Andreani, M. Agio, IEEE J. Quantum Electron. 38 (2002) 891.
[17] L.C. Andreani, Physica Status Solidi B 234 (2002) 129.
[18] L.C. Andreani, M. Agio, Appl. Phys. Lett. 82 (2003) 2011.
[19] V.N. Astratov, D.M. Whittaker, I.S. Culshaw, R.M. Stevenson, M.S. Skolnick, T.F. Krauss, R.M. De La Rue, Phys. Rev. B 60 (1999) R16255.
[20] D.M. Whittaker, I.S. Culshaw, Phys. Rev. B 60 (1999) 2610.
[21] A.R. Cowan, J.F. Young, Phys. Rev. B 65 (2002) 085106.
[22] S.G. Johnson, S. Fan, P.R. Villeneuve, J.D. Joannopoulos, L.A. Kolodziejski, Phys. Rev. B 60 (1999) 5751.